# Author response to referee #2

The authors thank Anonymous referee #2 for their comments on the manuscript. We will take the comments into account when revising the manuscript. In this document we provide responses to each of the referee's comments (formatted as italics in indented paragraphs). We respond to the referee's comments not in the order in which they are listed in the original comment, but in an order that improves the readability of this response.

> *Line 87: Vjet is defined between all SCs, but we can see from Figure 1, that velocity is different between the different THEMIS satellites. Also, what does "mean" value at t_max? isn't that 1 measurement, later it is suggested that it is the average value between the neighbor points, please clarify how the mean value is computed here.*

$V_{\mathrm{jet}}$ is calculated in the current manuscript as the mean value of one measurement of THA, THD and THE at their respective $t_{\max}$. We agree with the referee that THD observes a different velocity than THA and THE, as can be seen in Figure 1 in the current manuscript. The averaging over neighboring points was only done in Figure 2 to visualize the flow, not to estimate the propagation direction. In the revised manuscript, we will not average the velocities in order to make the paper easier to read. Moreover, the flow pattern is visible even without the averaging and we do not blur the measurements.

> *Line 87: Furthermore, the velocity of the jet can be higher in some cases than the moment product, since jets and the background population may co-exist (See Raptis et al. 2022), making the velocity observations having lower values in the data. How would a larger Vjet change your coordinate system there if you either take different measurements (pairs of SCs, maximum values, etc.) ? Also, if you assume that the velocity of the jet population is actually higher than measured due to non-Maxwellianity features (so maybe + 30-40%)?*

We agree with the referee that only considering the full moments may be error prone. Therefore we have repeated our analysis considering the velocity distribution (VDF) and included error treatment. We started with a closer look at the velocity distribution functions. A first glance, the 2D slices show only single maxima for THA, THD and THE, as shown in Figure 1.

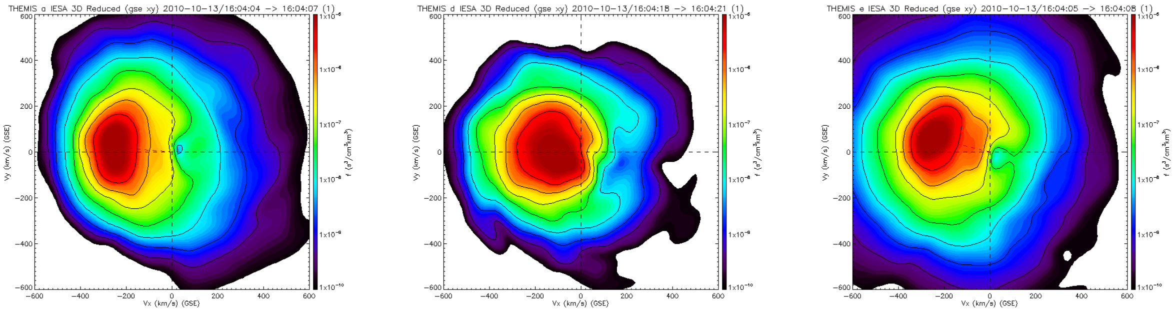

(a) THA (b) THD (c) THE

Figure 1: 2D slices of the velocity distribution around $t_{\max}$ in the $V_{\mathrm{X}} - V_{\mathrm{Y}}$ plane at $V_{\mathrm{Z}} = 0$.

For a more detailed look, we used the similar approach as Raptis et al. [2022] and integrated the 3D distribution over two velocity axes to get a 1D velocity distribution along the third component. The 1D distributions along GSE-$V_{\mathrm{X}}$, -$V_{\mathrm{Y}}$ and -$V_{\mathrm{Z}}$ at the time of maximum dynamic pressure ($t_{\max}$) are shown in Figures 2, 3 and 4 for THA, THD and THE, respectively.

Here, we were not able to see a clear bi-Maxwellian distribution for THA and THE in either of the three components. Instead, we observe individual peaks, albeit with deviations from the ideal Maxwellian distribution. For THD, we clearly see two maxima in the 1D distribution along $V_{\mathrm{Y}}$ and $V_{\mathrm{Z}}$.

Following the same conclusion as Raptis et al. [2022], THA and THE observe one plasma population. THD, which is also further away from the other two, observes two plasma populations, probably a mixture of jet and magnetosheath background plasma. Together with the lower dynamic pressure at $t_{\max}$, this suggests that THD is closer to the edge of the jet. To be conservative, we continued our analysis using only THA and THE to determine the direction of jet propagation. Furthermore, since we see that

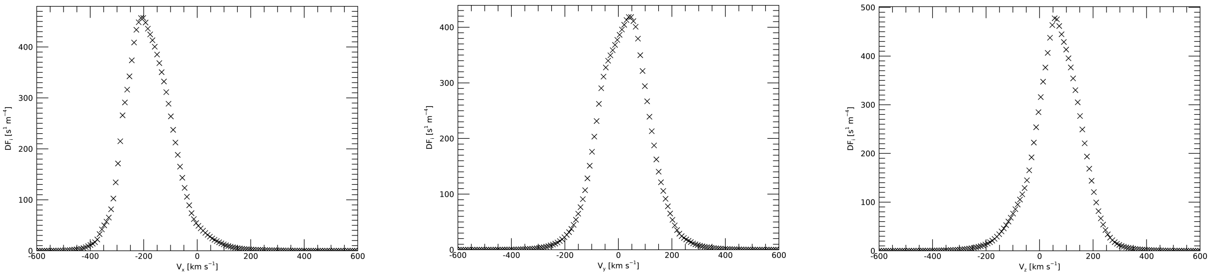

(a) THA - $V_{\mathrm{X}}$ (b) THA - $V_{\mathrm{Y}}$ (c) THA - $V_{\mathrm{Z}}$

Figure 2: 1D distribution from Integration along the other velocity axes.

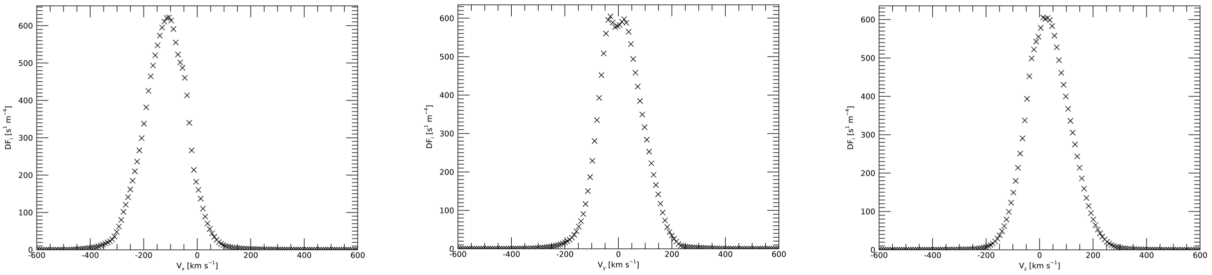

(a) THD - $V_{\mathrm{X}}$ (b) THD - $V_{\mathrm{Y}}$ (c) THD - $V_{\mathrm{Z}}$

Figure 3: 1D distribution from Integration along the other velocity axes.

the 1D VDFs at THA and THE deviate from ideal Maxwellians, we use the velocity at which the 1D VDF peaks in each component rather than the full plasma moments to determine the jet propagation direction. Other time steps inside the jet show similar 1D VDFs and outside the jet we observe 1D VDFs that look almost like ideal Maxwellians.
In the following (see figures 6 and 7) we will show that the coordinate system changes for different propagation directions, but we can still observe the diverging and converging flows.

> *Line 82-83: One direction vector is used, although it is very unlikely that it can fully characterize the direction. How does the result change if you use direction vectors taken from only one of the spacecraft or different pairs of them?*
> *Line 110: Here it is assumed that the propagation direction again is constant. This is not very likely to be the case as far as I am aware. How would this assumption change the result if it is not applicable? It would be nice to at least comment on that if quantification is not possible.*

We agree that one vector without uncertainty handling is not a good estimation of the propagation direction. We therefore investigated the stability of the direction of the jet velocity. Using the updated velocity values, we calculated the polar angle $\Theta$ ($= \arccos \frac{V_z}{\sqrt{V_x^2+V_y^2+V_z^2}}$) and the azimuthal angle $\varphi$ ($= \mathrm{sgn}(\mathrm{V_y}) \cdot \arccos \frac{V_x}{\sqrt{V_x^2+V_y^2}}$) of the measured velocities and plotted them over time. The results are

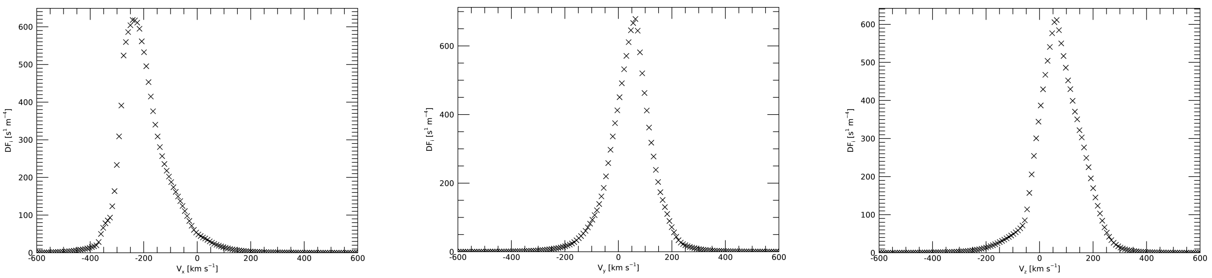

(a) THE - $V_{\mathrm{X}}$ (b) THE - $V_{\mathrm{Y}}$ (c) THE - $V_{\mathrm{Z}}$

Figure 4: 1D distribution from Integration along the other velocity axes.

shown in Figure 5a for all three spacecraft (for completeness, THD is also shown).

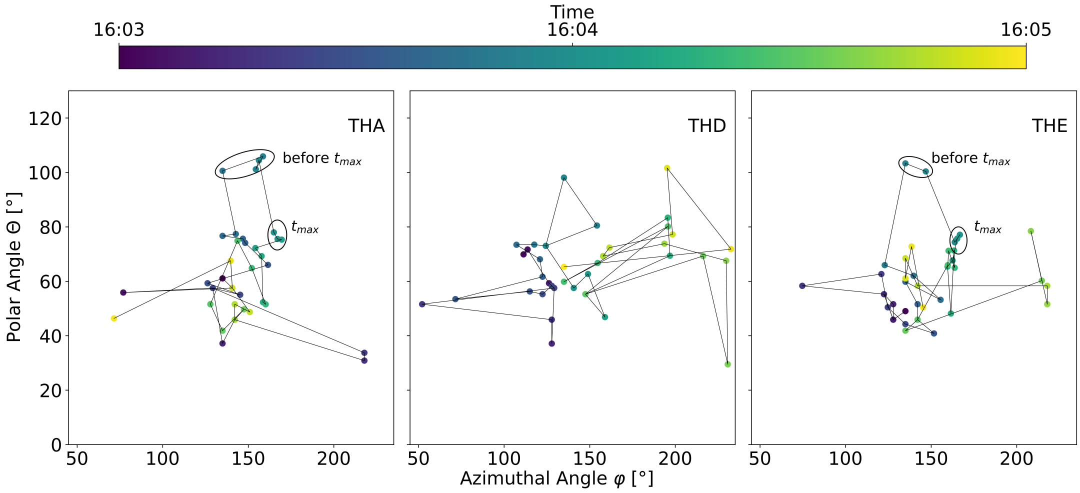

(a) Time evolution of measured velocity direction over time for THA, THD and THE in the columns from left to right. The time is color coded with darker colors corresponding to earlier times and lighter colors corresponding to later times. The polar angle Θ and the azimuthal angle $\varphi$ are described in the text.

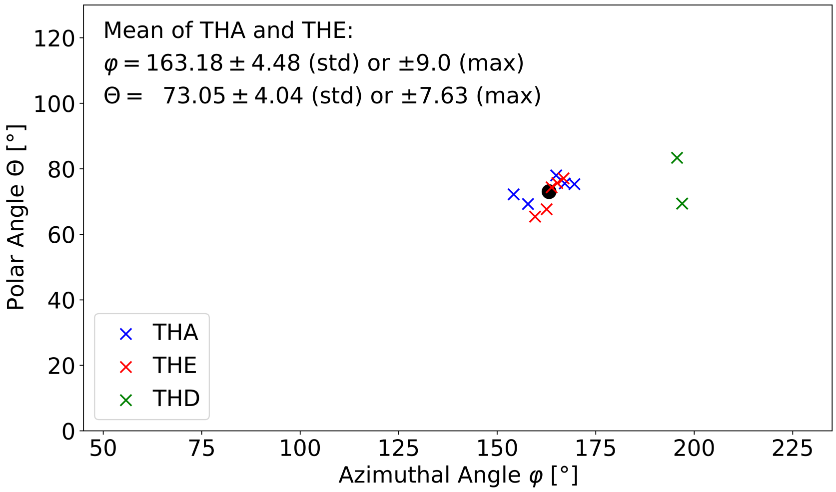

(b) Velocity direction around $t$max from THA, THD and THE in red, green and blue, respectively. The black dot corresponds to the mean value of the measurements from THA and THE.

Figure 5: Determination of propagation direction.

Here, we also observe a rather turbulent behavior at THD. For THA and THE, on the other hand, we see that Θ and $\varphi$ are constant around $t_{\max}$ (marked with black circle). To obtain a direction for the jet velocity, we determined the mean value of Θ and $\varphi$ of the velocities measured by THA and THE around $t_{\max}$.
This is shown in Figure 5b. For comparison, we have also plotted the direction of THD, but we can clearly see that it deviates strongly from THA and THE. As an error, we have calculated the standard deviation and also the maximum difference in Θ and $\varphi$. To be conservative, we use the maximum difference in Θ and $\varphi$ from the mean for error handling in the following analysis.

> *Line 94: Here the choice of 12 seconds before and after the tmax is not clear. Isn't that time within the jet observation itself since the duration of the jet is larger than that? Wouldn't that mean that for Figure 2 we just see the jet observations rather than the "before" and "after" periods of the jet flow? Something is unclear here.*
> *Line 102-103: Again here, you are referring to an evasive motion, but shouldn't that occur "after" the jet observations? if that's only 12 seconds after tmax, aren't these observations still*

*referring to the jet itself, and not the plasma after its passage?*

The referee is absolutely right that the analyzed flow is inside the jet structure, and we thank the referee for pointing out the misleading description. Nevertheless, Plaschke and Hietala [2018] have shown that the evasive motion is also present inside the jet. Therefore, we should expect the same behavior with a diverging flow before and a converging flow after $t_{\max}$.

With the focus on the flow behavior within the jet, we saw the need to change our transformation to the jet coordinate system. The transformation involves only a simple rotation. We use the estimated propagation direction as the new $\mathbf{X'}$ axis and no longer subtract the background velocity. There are two reasons for this. Firstly, we only want to consider the velocity perpendicular to the propagation direction. Secondly, we do not see a bimaxwellian distribution (for THA and THE) and assume that the spacecraft observe almost exclusively the jet plasma.

We calculated $\boldsymbol{Y'}\left(=\frac{\boldsymbol{X'}\times\hat{\boldsymbol{X}}}{|\boldsymbol{X'}\times\hat{\boldsymbol{X}}|}\right)$ and $\boldsymbol{Z'}=\left(\frac{\boldsymbol{X'}\times\boldsymbol{Y'}}{|\boldsymbol{X'}\times\boldsymbol{Y'}|}\right)$ in the same way as described in the current manuscript, and we rotate the measured velocities and the positions of the spacecraft into the new coordinate system. The origin of our new coordinate system was chosen arbitrary to be at the position of the THA at $t_{\max} = [X = 10.76R_{\mathrm{E}}, Y = 0.34R_{\mathrm{E}}, Z = 1.49R_{\mathrm{E}}]$ (in GSE coordinates). The results are shown in Figure 6 for the velocities determined from the peaks in the 1D VDFs and in Figure 7 for the velocities from the full moments for comparison. The middle rows in both figures show the resulting flow pattern when the mean jet propagation direction (see Figure 5b) is used. The bottom (top) rows of both figures show the resulting flow pattern when the errors are subtracted from (added to) the mean jet propagation direction.

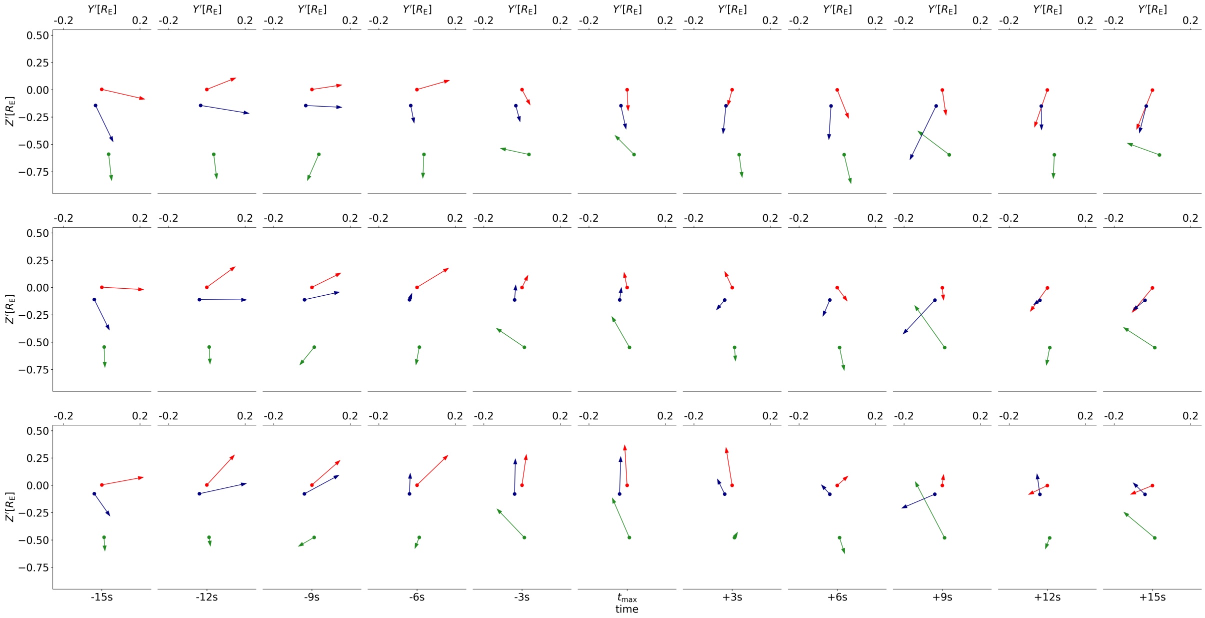

Figure 6: Flow pattern inside the jet around $t_{\max}$ with velocities from 1D-VDFs. Dots (arrows) in red, green and blue represent the position (measured velocity) of THA, THD and THE, respectively. The middle row represent the resulting flow pattern when the mean jet propagation direction is used. The bottom (top) row shows the resulting flow pattern when the errors are subtracted from (added to) the mean jet propagation direction.

We continue to consider only THA (red arrows) and THE (blue arrows), as we have already mentioned that THD observes a mixture of plasma populations. We see in all cases in the time from -15s to -6s signs of diverging velocity vectors before $t_{\max}$. Around -3s to +9s, we observe high dynamic pressure (see Figure 1 in the current manuscript) and a more complex flow pattern. After $t_{\max}$ from +12s to +15s, we observe signs of the converging pattern, again in almost all cases. This should indicate the applicability of our approach even for a non-perfectly estimated propagation direction.

Furthermore, we estimated the position of the center of our jet from the diverging and converging flow at THA and THE. Figure 8 shows the temporal evolution of the center position for flow patterns determined from 1D VDFs and full moments. As we can see, the deviation of the center position is relatively small in both cases (except for errors added - top rows). In addition one can see that the center position is

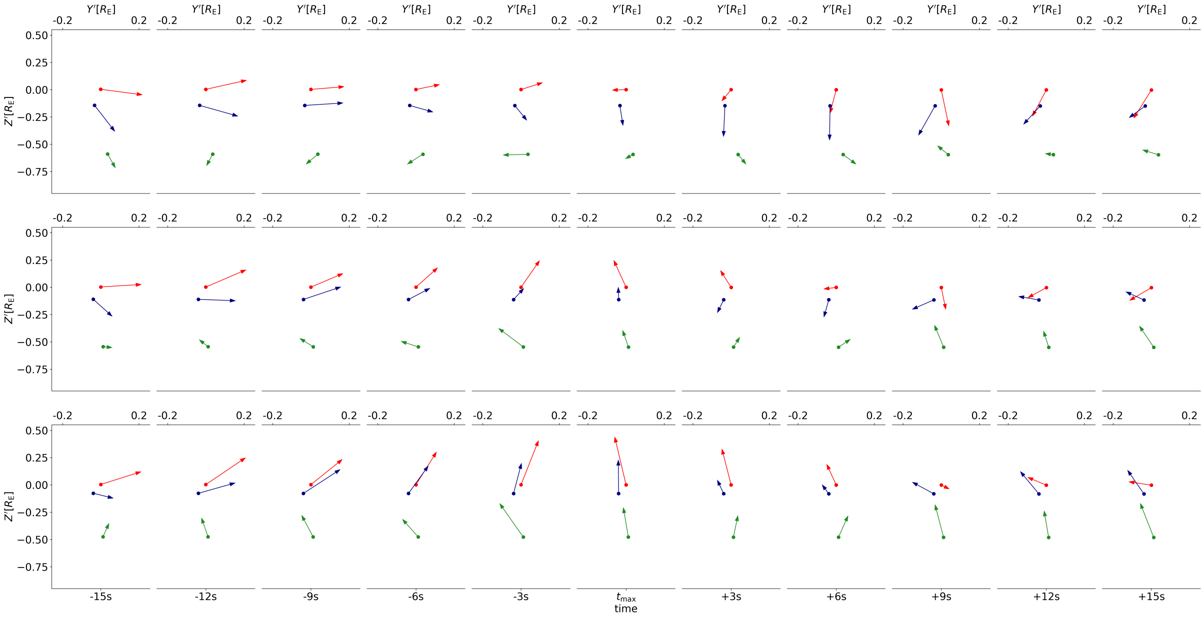

Figure 7: Flow pattern inside the jet around $t_{\max}$ with velocities from full moments. Dots (arrows) in red, green and blue represent the position (measured velocity) of THA, THD and THE, respectively. The middle rows represent the resulting flow pattern when the mean jet propagation direction is used. The bottom (top) row shows the resulting flow pattern when the errors are subtracted from (added to) the mean jet propagation direction.

more stable when we use the velocities from the 1D-VDFs.
In the revised version of the manuscript we will alter the introduction and methodology accordingly and describe the new transformation together with the uncertainty treatment. We also want to point out that only two spacecraft could suffice to estimate the center of the jet.

> *Line 86: Mean velocity is defined as the average velocity of a very large window, which is also not compared if it is similar between all SCs. Also, if there is variability due to the presence of other flows this should also be affected and we can actually see THD measuring a flow increase at 16:02, almost above the threshold given in dynamic pressure. How would your result change if you remove the jet observations and other potential fast flows or if you change the window you average through?*

The referee correctly points out that fast flows in the near jet environment have a strong influence on the calculated background flow. Using only quiet times (without increased dynamic pressure values), the background flow is reduced by 16% and rotates by 13°. However, since we will use a slightly different transformation, we no longer need the background flow.

> *Line 95: This is the first time the word "center" is used, dropped abruptly without much explanation as to what it means or how it is derived. Some re-structuring and clarification could be useful here.*

We agree that we have to rewrite the introduction and methodology according the updated analysis and with a structure that can be easier followed.

> *Readability of the paper: My overall suggestion here is to restructure section 2 and 3 to form clearer sections. Presently, neither of these sections are clearly separated, which forces the reader to go back and forth between the sections to understand what you are trying to say. For example, Figure 2 is only mentioned in the data and methods section, but then it is presented as part of the results in the discussion. The Gaussian fit is suddenly mentioned in the result section, which should have been mentioned before. Also, the motivation for this fit profile should have been made in the data and methods section, but currently it is shown at the end of the*

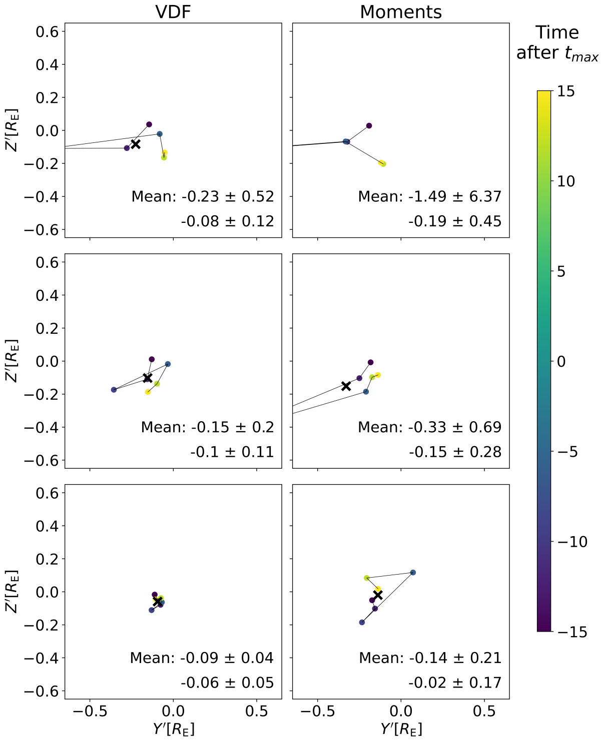

Figure 8: Time evolution of center position from the flow patterns with velocities from the 1D-VDFs (left column) and from the full moments (right column). The middle row represent the results when the mean jet propagation direction is used. The bottom (top) row shows the results when the errors are subtracted from (added to) the mean jet propagation direction.

> *discussion (lines 168-173)! A re-organizing of such aspects could greatly improve the readability of the paper.*

We agree that the structure of the paper needs to be revised. In the revised version of the manuscript, we will focus on a more consistent structure that should be easier for the reader to follow.

> *Figure 2: You mention that the top axis shows the Y' coordinate, while the Z' is constant. However, the values shown on the top x-axis appear to be constant on every time step. Could you explain a bit more what we are seeing here?*

The $Y'$ axis is also the same for each time step. In contrast to the $Z'$ axis, we have plotted the $Y'$ axis separately for each time step, so that the reader can in principle see the actual positions of the spacecraft in the flow chart. We recognize the need to describe the figure in a better way and will do so in the revised manuscript.

> *Lines 177-180: These two results, appear to be driven by the definition of a jet and the methodology itself. In other words, Tmax will automatically drive a dynamic pressure higher, since, well, the fit parameters at t_max have as input higher dynamic pressure pairs, so Po will be higher. Is that correct? Do I miss something? Also, the same applies for $\Delta R$. According to my understanding, this will be the cause for every jet that has a single peak in dynamic pressure (and therefore lower values before and after it). Could you either help me understand if I miss something here, or describe a hypothetical (or real) case for which your methodology would not result always in the same conclusion*

From the measurement of a single spacecraft one can't say anything about the jet shape as the region and direction how the spacecraft traverses the jet has a great influence on the measurement. With our methodology we try to gather more information about the shape of the jet from two or more spacecraft measurements. The shape of jets is still under debate and as shown in Figure 9 there are in principle multiple possibilities for the jet shape. In the Figure, in all columns the darkest color correspond to a fit at $t_{\max}$ and lighter colors correspond to later times ($t_{\max} < t_1 < t_2$). Case a) belongs to a jet which has its largest expansion around $t_{\max}$. The expansion decreases towards the front and rear parts of the jet, while the dynamic pressure stays constant. In b) one can see the opposite case with constant expansion of the jet. The dynamic pressure is highest around $t_{\max}$ and decreases toward front and rear parts. In c) both dynamic pressure and expansion are highest around $t_{\max}$ and decrease before and afterwards. While we don't expect a) to be a realistic, we are can't say for sure from a single spacecraft measurement which of the cases describes the jet shape. In addition, we also wanted to point out that statistical studies on magnetosheath jets systematically underestimate the dynamic pressure as spacecraft rarely observe the center of jets.

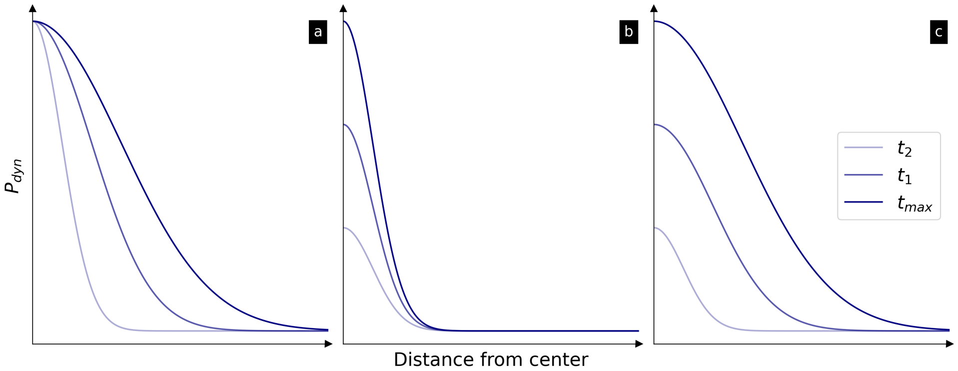

Figure 9: Hypothetical fits to dynamic pressure measurements plotted against distance from center for three different scenarios of jet shapes. In all columns fits for three different times (= different intersections of the jet) are shown. The darkest color correspond to a fit at $t_{\max}$ and lighter colors correspond to later times ($t_{\max} < t_1 < t_2$). The shown cases are described and explained in the text.

We realize that we need to rewrite the last section to more clearly present our conclusion to the reader.

> *Line 2: Not all jets are formed at the bow shock, maybe such a general statement shouldn't be in the abstract.*
> *Line 3-6: This sentence is very hard to read, consider splitting it.*
> *Line 13 and throughout the text: Consider changing Θ to Θ_Bn since that's the typical symbol used.*

We agree with the referee and revise the manuscript accordingly.

# References

Plaschke, F. and Hietala, H. (2018). Plasma flow patterns in and around magnetosheath jets. *Ann. Geophys.*, 36(3):695–703. doi: 10.5194/angeo-36-695-2018.

Raptis, S., Karlsson, T., Vaivads, A., Lindberg, M., Johlander, A., and Trollvik, H. (2022). On magnetosheath jet kinetic structure and plasma properties. *Geophysical Research Letters*, 49(21):e2022GL100678. doi: 10.1029/2022GL100678.